# Stability Analysis of Vector-Controlled Modular Multilevel Converters in Linear Time Periodic Framework

Nilanjan Ray Chaudhuri, *Member, IEEE*, Rafael Oliveira, and Amirnaser Yazdani, *Senior Member, IEEE*

***Abstract*—Stability analysis of average value models (AVMs) of vector-controlled Modular Multilevel Converters (MMCs) is the subject matter of this paper. Stability analysis of fundamental frequency phasor-based AVMs of MMCs can be conducted in a traditional linear time-invariant (LTI) framework through eigenvalue computation. This class of models do not consider circulating current control loop and hence fails to capture system instability that occurs in a certain range of gains of the circulating current controller. We propose stability analysis in a linear time-periodic (LTP) framework to solve this issue. To that end, a nonlinear AVM is presented that considers the submodule (SM) capacitor insertion dynamics and takes into account the output and the circulating current control schemes in vector control approach. Upon linearization, an LTP model is derived from this averaged model. It is shown that the Poincaré multipliers are indicative of system instability corresponding to a certain range of gains of the circulating current controller.**

***Index Terms*—Linear Time Periodic, Linear Time Varying, Modular Multilevel Converter, Stability, State Transition Matrix.**

## I. Introduction

THE Modular Multilevel Converter (MMC) has gained immense popularity since it was invented [1], [2]. The focus of this paper is on the stability analysis of average value models (AVMs) of MMCs. It presents a comprehensive stability analysis framework for MMCs under closed-loop control that takes into account the circulating current control loops and the output current control loops. As an example, vector control, which is popular in the industry, is considered as the control methodology. The proposed analytical approach is critical in developing insight into the zones of stability of MMC controller gains, and therefore, can have significant theoretical and practical importance.

Literature review shows that a lot of attention has been focused on the modeling and control of MMCs [3] - [30]. On the contrary, only a few papers [31] - [34] presented stability analysis framework of the MMC. We divide the literature into two parts: (A) papers that presented only modeling and control philosophy, and (B) papers that presented stability analysis. In the following sections, we will conduct a comprehensive review of this literature in order to distinguish our contribution.

N. R. Chaudhuri is with Department of Electrical & Computer Engineering, North Dakota State University, Fargo, ND, USA (e-mail: *nilanjan-ray.chaudhur@ndsu.edu*).

R. Oliveira and A. Yazdani are with Department of Electrical & Computer Engineering, Ryerson University, Toronto, ON, Canada (e-mail: *rafael.oliveira@ryerson.ca*, *yazdani@ryerson.ca*).

Financial support from NSF ND EPSCoR New Faculty Startup Grant (Award # FAR0021960) is gratefully acknowledged.

### A. Literature on MMC Modeling & Control

Xiaofeng et-al [3] proposed a model to represent the circulating current in the MMC. The paper did not include the controllers in their model and did not present any framework for stability analysis. Kolb et-al [4] focused on a novel control strategy for MMCs, which allows feeding a three-phase machine over its complete frequency range. Two operating modes were proposed in this paper: a low frequency mode for startup and low speed operation, and a high frequency mode for higher speeds. The same authors proposed a cascaded control system for MMCs for variable-speed drives [5]. The decoupled current control strategy proposed in this paper transforms the $abc$ frame quantities into $\alpha\beta 0$ quantities for the phase currents and the circulating currents (referred as 'e' currents). The proposed control system ensures a dynamic balancing of the energies in the MMC cells at minimum internal currents over the complete frequency range. However, none of these papers presented a comprehensive modeling framework that can be used for stability analysis of MMCs. Munch et-al [6] wrote a very important paper that showed that MMC can be modeled as a periodic bilinear time-varying system capturing all currents and energies. It assumed that the submodule (SM) capacitor voltages are balanced and focused on horizontal and vertical energy balancing among the group of phase modules (PMs). The state-space model, although insightful, leads to a control design that requires a p-periodic Linear Quadratic Regulator (PLQR), which possesses periodic time-varying gains. No obvious advantage was established over the existing constant gain controllers that are more popular due to their simplicity. Moreover, the paper did not offer any insight into the stability analysis using such models. Reference [7] proposed a Linear-Time-Invariant (LTI) state-apace model of the MMC, which is not adequate to analyze the interaction between the circulating current control and output current control loops.

Siemaszko et-al [8] presented a comparison between four modulation strategies in MMCs. These strtegies are: direct modulation, closed-loop control, open-loop control and Phase-shifted Carrier-based Pulse-width modulation (PSCB-PWM). Similar analysis was also reported in [9]. A fundamental-frequency control of the circulating current of the MMC was proposed in [10]. Although these three papers focus on different control methodologies of MMC, they do not present

any modeling and stability analysis. A nonlinear switching function-based model of MMC was presented in [11], which was used for time-domain simulation. Marcelo et-al presented a model of the MMC based on switching function-driven controllable voltage sources in [12] and proposed a vector control strategy in [13] for output current control, circulating current control, and average dc voltage control. Unfortunately, due to the switched nature of the model, it is not straightforward to do stability analysis. Yan et-al [14] presented an averaged model in rotating $d-q$ reference frame. The model is oversimplified and does not consider circulating current. Stefan et-al [15] proposed the reduction of cell capacitance by injecting harmonic current in the circulating current. Steffen et-al [16], [17] presented a nonlinear time-varying state-space AVM of MMCs. The model described in [17] is of particular interest, and has some similarities with the model developed in this paper. The key difference however, is that, in this paper the closed loop control is also considered within the model. More importantly, an approach for stability analysis has also been presented in our paper, which was not done in [17]. Many other papers including [18] - [26] also focused on modeling and control of MMCs without considering any framework for stability analysis. Teeuwsen et-al [27] presented a positive-sequence fundamental frequency model of MMCs for phasor simulation with large AC systems. This model cannot capture the circulating current and corresponding control loops. A fundamental frequency AVM, called the Type 6 model, was reported in [28] and [29]. These models can also be used for phasor-based simulations. In this paper, we shall call such models 'phasor-based AVMs.' Phasor-based AVMs neglect the dynamics of the submodule (SM) capacitors and, therefore, do not capture the circulating current. Upon linearization, this class of models can be treated as linear time-invariant (LTI) and traditional eigenvalue analysis can be performed to ascertain stability. We will demonstrate that there are different regions of gains of the circulating current controller that can destabilize the MMC. Since the phasor-based AVMs do not consider the circulating current control loop, it can not indicate such instability. The objective of this work is to present a modeling and stability analysis framework that solves this problem.

It is important to note that the operating principle of MMCs is fundamentally different from other VSC topologies. Unlike the conventional VSC topologies (e.g., 2 or 3-level), the MMC operates based on *physical modification* of its circuit, i.e., insertion and bypassing of its SMs in a discrete manner. The AVM presented in [30] approximates the SM insertion and bypassing as a continuous function, and, thus, captures the circulating currents flowing through the arms.

### B. Literature on Stability Analysis of MMC

Although a lot of work has been done on the modeling and control aspect of MMCs, very little has been reported on establishing a comprehensive stability analysis framework of MMCs that considers closed-loop control, e.g. vector control approach. The global asymptotic stability of MMCs was analyzed in [31], which did not consider any closed-loop control strategy for stability analysis. In [32] and [33], the authors studied the stability of the MMC as an open-loop system. They made multiple simplifying assumptions to convert the linear time-varying (LTV) model into an LTI model. Hagiwara et-al [34] used Routh-Hurwitz stability criterion for conducting stability analysis of one arm of the MMC converter where only the circulating current was considered as the state variable.

### C. Motivation, Contribution & Application of this paper

In view of the above literature review, it is clear that

- Papers that presented stability analysis of MMCs either modeled systems under open-loop conditions or made quite a few simplifying assumptions to avoid complexities of a rigorous stability analysis.
- A modeling framework of MMCs considering closed-loop control, which is suitable for stability analysis, has not been presented.
- An analytical method for rigorous stability study is necessary. It will be shown in this paper that traditional eigenvalue analysis fails to detect the regions of instability of MMCs under closed-loop control.

The AVM introduced in this paper, while complex, considers the closed-loop control system in the modeling framework. Moreover, it presents a rigorous stability analysis approach without simplifying assumptions.

The key contributions of this paper are:

- It presents a comprehensive modeling framework that augments the AVM that considers SM insertion dynamics with widely-used vectorial control for the output current control loop and the circulating current control loop.
- It proposes a stability analysis methodology of MMCs in a linear time-periodic (LTP) framework.
- It demonstrates through case studies that the proposed approach can indicate a range of compensator gains of the circulating current control scheme which can destabilize the MMC.

The proposed analytical approach is critical in developing insight into the zones of stability of MMC controller gains, and therefore, can have significant theoretical and practical importance. It should be mentioned that the proposed technique is applicable for any control philosophy (not limited to vector control), as long as the closed-loop system can be represented in the form of an LTP model.

## II. Overview of MMC Control System

Figure 1 shows a circuit diagram of the $j^{th}$ phase of an MMC. The MMC is connected to the host ac system through a transformer represented by its series resistance and leakage inductance. The MMC control system has three key functionalities:

- *Balancing Control:* The capacitor voltages across all SMs shown in Fig. 1 must be balanced and kept equal. Different voltage balancing techniques have been proposed in literature, e.g. [35] - [42].
- *Circulating Current Control:* Second harmonic circulating current originates from unbalance in the arm voltages.

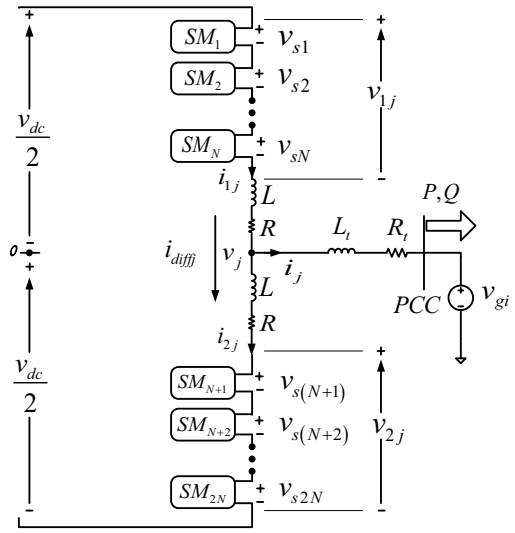


Fig. 1. Schematic of the $j^{th}$ phase ($j = a, b, c$) of the MMC.

This distorts the arm current and increases the dc voltage ripple in SMs. References [43] - [48] are a few papers from the vast literature in this area that have proposed circulating current control strategies.

- *Output Current Control:* The output current or phase currents are not affected by the circulating current and can be controlled by decoupled current control approach.

Throughout this paper, it is assumed that the voltages across all the SMs are balanced and the dc-side voltage $v_{dc}$ is constant.

## III. Phasor-based AVM of MMC

The phasor-based AVM [28] is derived with the following assumptions:

- SM capacitor insertion dynamics is neglected.
- Second harmonic circulating current is completely suppressed.
- The model is derived in a synchronously rotating $d-q$ reference frame assuming no harmonic content in the arm voltages $v_{1j}$ and $v_{2j}$.

From Fig. 1, applying KCL in phase $j$, one obtains

$$\begin{aligned} i_{1j} &= \frac{i_j}{2} + i_{diffj} \\ i_{2j} &= -\frac{i_j}{2} + i_{diffj} \end{aligned} \tag{1}$$

Applying KVL in phase $j$ one obtains

$$\begin{aligned} v_{dc} - v_{1j} - v_{2j} &= 2L\frac{di_{diffj}}{dt} + 2Ri_{diffj} \\ \frac{v_{2j}}{2} - \frac{v_{1j}}{2} - v_{gj} &= L'\frac{di_j}{dt} + R'i_{1j} \end{aligned} \tag{2}$$

where $L' = L_t + \frac{L}{2}$, and $R' = R_t + \frac{R}{2}$. As shown in Fig. 1, $v_{1j}$ and $v_{2j}$ are the voltages across the upper and the lower arm SMs that are in *on-state*.

As mentioned before, the second harmonic component of the circulating current is assumed to be perfectly suppressed. Expressing the second equation of (2) in a synchronously rotating $d-q$ reference frame, one can write:

$$\begin{aligned} L'\frac{di_d}{dt} &= -R'i_d + L'\omega i_q + e_d - v_{gd} \\ L'\frac{di_q}{dt} &= -R'i_q - L'\omega i_d + e_q - v_{gq} \end{aligned} \tag{3}$$

where, $e_d = \frac{v_{2d}-v_{1d}}{2}$, $e_q = \frac{v_{2q}-v_{1q}}{2}$. We consider widely-used vector control strategy for the output current control loop, which is described next.

### A. Vector Control: Output Current Control Scheme

A VSC is commonly current-controlled through a vectorial control strategy in a rotating $d-q$ reference frame [49]. Figure 2 shows the current control scheme of the MMC in the $d-q$-frame with the decoupling feed-forward signals. A Phase-Lock-Loop (PLL) ensures that the $d$-axis of the rotating $d-q$ reference frame is aligned with the grid voltage vector $\vec{v}_g$.

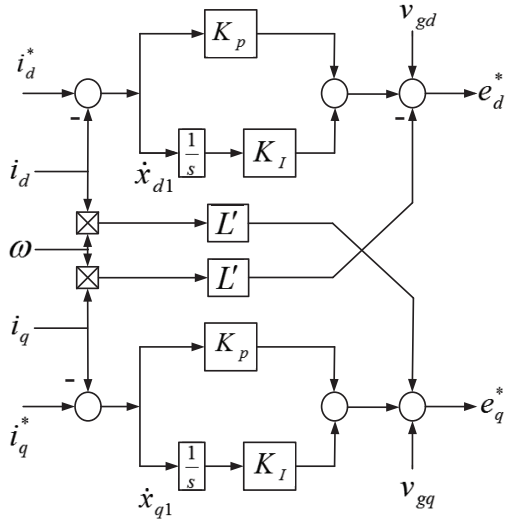


Fig. 2. The current control scheme of the MMC in a rotating $d-q$ frame of reference.

As Fig. 2 indicates, the reference voltage commands in the $d-q$ frame are given by

$$\begin{aligned} \begin{bmatrix} e_d^* \\ e_q^* \end{bmatrix} &= K_p \begin{bmatrix} i_d^* \\ i_q^* \end{bmatrix} - K_p \begin{bmatrix} i_d \\ i_q \end{bmatrix} + K_I \begin{bmatrix} x_{d1} \\ x_{q1} \end{bmatrix} \\ &+\omega L' \begin{bmatrix} -i_q \\ i_d \end{bmatrix} + \begin{bmatrix} v_{gd} \\ v_{gq} \end{bmatrix} \end{aligned} \tag{4}$$

where $x_{d1}$ and $x_{q1}$ are the state variables of the Proportional-Integral (PI) compensators in the $d-q$ frame. The $d$ and $q$-axis components of the ac grid voltage vector $\vec{v}_g$ and those of the current $\vec{i}$ are denoted by $v_{gd}$, $v_{gq}$, $i_d$, and $i_q$, respectively. The state-space equations of the PI compensators can be written as

$$\begin{bmatrix} \dot{x}_{d1} \\ \dot{x}_{q1} \end{bmatrix} = \begin{bmatrix} i_d^* \\ i_q^* \end{bmatrix} - \begin{bmatrix} i_d \\ i_q \end{bmatrix} \tag{5}$$

It is assumed that the converter delay is negligible and the following control law as described in [43] is considered:

$$e_d = e_d^* = \frac{v_{2d} - v_{1d}}{2}, e_q = e_q^* = \frac{v_{2q} - v_{1q}}{2} \tag{6}$$

### B. State-space Model of Phasor-based AVM

Combining equations (3), (4), (5), and (6) one can write the phasor-based AVM in the following state-space form:

$$\begin{bmatrix} \dot{i}_d \\ \dot{i}_q \\ \dot{x}_{d1} \\ \dot{x}_{q1} \end{bmatrix} = \begin{bmatrix} -\frac{K_p+R'}{L'} & 0 & \frac{K_I}{L'} & 0 \\ 0 & -\frac{K_p+R'}{L'} & 0 & \frac{K_I}{L'} \\ -1 & 0 & 0 & 0 \\ 0 & -1 & 0 & 0 \end{bmatrix} \begin{bmatrix} i_d \\ i_q \\ x_{d1} \\ x_{q1} \end{bmatrix} + \begin{bmatrix} \frac{K_p}{L'} & 0 \\ 0 & \frac{K_p}{L'} \\ 1 & 0 \\ 0 & 1 \end{bmatrix} \begin{bmatrix} i_d^* \\ i_q^* \end{bmatrix} \tag{7}$$

It can be seen that this model has 4 state-variables and 2 control variables. Next, we will discuss the stability analysis of the same.

## IV. Stability Analysis: Phasor-based AVM

Equation (7) shows that

- The model is linear time-invariant (LTI) in nature
- The state matrix is independent of the circulating current controller gains

Traditional eigenvalue computation can be performed to analyze the stability of this system. Clearly, any instability caused by the circulating current controller will not be captured. In Section VII, we will do eigenvalue analysis for a test system to highlight this point.

This sets up the motivation for developing a comprehensive modeling and stability analysis framework that will be able to solve such issues.

## V. Proposed AVM of MMC Considering SM Insertion Dynamics

Unlike the phasor-based AVM, the insertion of SM capacitances was considered in this model, as proposed in [30]. In practice, the change in the total capacitance of one arm of the converter shown in Fig. 1 will happen in a discrete manner. As the number of SMs increase, this variation can be *approximated using a continuous function.*

Let $\eta_{Uj}^*$ and $\eta_{Lj}^*$ denote the fractions of the total number of SMs in the upper and the lower arm of phase $j$, which are in *on-state*. Variables $\eta_{Uj}^*$ and $\eta_{Lj}^*$ are control commands, which are obtained from the output current control scheme and the circulating current control scheme. Since $C$ is the capacitance of each SM and $N$ is the total number of SMs in each arm, the equivalent capacitance of the modules in *on-state* is given by $\frac{C}{N\eta_{Uj}^*}$ for the upper arm and $\frac{C}{N\eta_{Lj}^*}$ for the lower arm. The capacitor voltage dynamics of the upper and the lower arm SMs of phase $j$ can be written as

$$\begin{aligned} \frac{C}{N\eta_{Uj}^*}\frac{dv_{Uj}}{dt} &= i_{1j} \\ \frac{C}{N\eta_{Lj}^*}\frac{dv_{Lj}}{dt} &= i_{2j} \end{aligned} \tag{8}$$

where $v_{Uj}$ and $v_{Lj}$ are the voltages across all SMs in the upper arm and the lower arm of the $j^{th}$ phase, respectively.

In this work, the dc-side voltage $v_{dc}$ is assumed constant. From (1), (2), and (8) a nonlinear AVM can be formulated for the MMC, as:

$$f_{1j} = \frac{dv_{Uj}}{dt} = \frac{N}{C}\left(\frac{i_j}{2} + i_{diffj}\right)\eta_{Uj}^* \tag{9}$$

$$f_{2j} = \frac{dv_{Lj}}{dt} = \frac{N}{C}\left(-\frac{i_j}{2} + i_{diffj}\right)\eta_{Lj}^* \tag{10}$$

$$f_{3j} = \frac{di_{diffj}}{dt} = \frac{1}{2L}\left(v_{dc} - 2Ri_{diffj} - \eta_{Uj}^* v_{Uj} - \eta_{Lj}^* v_{Lj}\right) \tag{11}$$

$$f_{4j} = \frac{di_j}{dt} = \frac{1}{L'}\left(-v_{gj} - R'i_j + \frac{\eta_{Lj}^* v_{Lj}}{2} - \frac{\eta_{Uj}^* v_{Uj}}{2}\right) \tag{12}$$

We shall proceed from where we left in Section III-A and develop the framework for including the output current control scheme into our model, which is described next.

### A. Vector Control: Output Current Control Scheme

Continuing from where we were in Section III-A, let the ac system phase voltages be

$$\begin{aligned} v_{ga} &= V_{gm}\cos\omega t \\ v_{gb} &= V_{gm}\cos\left(\omega t - \frac{2\pi}{3}\right) \\ v_{gc} &= V_{gm}\cos\left(\omega t - \frac{4\pi}{3}\right) \end{aligned} \tag{13}$$

Assuming $\rho = \omega t$, the reference voltage corresponding to phase $a$ can be derived as:

$$e_a^* = \begin{bmatrix} \cos\rho & -\sin\rho \end{bmatrix}\begin{bmatrix} e_d^* & e_q^* \end{bmatrix}^T \tag{14}$$

Pre-multiplying (4) by $\begin{bmatrix} \cos\rho & -\sin\rho \end{bmatrix}$, we get:

$$\begin{aligned} e_a^* = K_p\left\{i_d^*\cos\rho - i_q^*\sin\rho\right\} - K_p i_a + K_I x_{a1} + v_{ga} \\ - \omega L'\left\{i_d\sin\rho + i_q\cos\rho\right\} \end{aligned} \tag{15}$$

where $x_{a1} = \begin{bmatrix} \cos\rho & -\sin\rho \end{bmatrix}\begin{bmatrix} x_{d1} & x_{q1} \end{bmatrix}^T$. We assume that no zero-sequence current can flow in the system, i.e.,

$$i_a + i_b + i_c = 0 \tag{16}$$

With this assumption, we can write:

$$i_d\sin\rho + i_q\cos\rho = \frac{1}{\sqrt{3}}\left(i_b - i_c\right) = \frac{1}{\sqrt{3}}\left(i_a + 2i_b\right) \tag{17}$$

Keeping the identities of the reference input quantities $i_d^*$ and $i_q^*$, one can derive the equation for $e_a^*$ as

$$e_a^* = K_p\left(i_d^*\cos\rho - i_q^*\sin\rho\right) - \left(K_p + \frac{\omega L'}{\sqrt{3}}\right) i_a + K_I x_{a1} + v_{ga} - \frac{2\omega L'}{\sqrt{3}} i_b \tag{18}$$

It can be observed that the voltage reference $e_a^*$ is cross-coupled with phase-$b$ current. Fundamentally, this coupling implies that the reference voltage of one phase is not only determined by the voltage, current, and PI-controller state variable of that phase, but also by the current of the other phase.

Following similar steps, the reference voltage for phase-$b$ can be derived as

$$e_b^* = K_p\left\{i_d^*\cos\left(\rho - \frac{2\pi}{3}\right) - i_q^*\sin\left(\rho - \frac{2\pi}{3}\right)\right\} - \left(K_p - \frac{\omega L'}{\sqrt{3}}\right) i_b + K_I x_{b1} + v_{gb} + \frac{2\omega L'}{\sqrt{3}} i_a \tag{19}$$

The voltage reference for phase-$c$ can be expressed in terms of those of phase $a$ and $b$. Therefore, from now on, only the models for phases $a$ and $b$ will be analyzed.

The state-space model of the PI compensators in a synchronously rotating $d-q$ reference frame was described in equation (5). Transforming the $d$-$q$ frame quantities to phase quantities, one obtains

$$f_{5a} = \frac{dx_{a1}}{dt} = -\frac{\omega}{\sqrt{3}}\left(x_{a1} + 2x_{b1}\right) - i_a + \left(i_d^*\cos\rho - i_q^*\sin\rho\right) \tag{20}$$

$$f_{5b} = \frac{dx_{b1}}{dt} = \frac{\omega}{\sqrt{3}}\left(2x_{a1} + x_{b1}\right) - i_b + i_d^*\cos\left(\rho - \frac{2\pi}{3}\right) - i_q^*\sin\left(\rho - \frac{2\pi}{3}\right) \tag{21}$$

Equations (20) and (21) will be augmented with equations (9) through (12) while formulating the nonlinear state-space model described in Section V-D.

Next, we will include the circulating current controller in the model.

### *B. Vector Control: Circulating Current Control Scheme*

The circulating current [43], $i_{diffj}$, is given by

$$\begin{aligned} i_{diffa} &= \frac{i_{dc}}{3} + I_{2f}\cos\left(2\omega t + \varphi\right) \\ i_{diffb} &= \frac{i_{dc}}{3} + I_{2f}\cos\left(2\omega t + \varphi - \frac{4\pi}{3}\right) \\ i_{diffc} &= \frac{i_{dc}}{3} + I_{2f}\cos\left(2\omega t + \varphi - \frac{2\pi}{3}\right) \end{aligned} \tag{22}$$

The circulating current is controlled in a $d-q$ reference frame that rotates with an angular speed of $2\omega$ [43], as Fig. 3 illustrates.

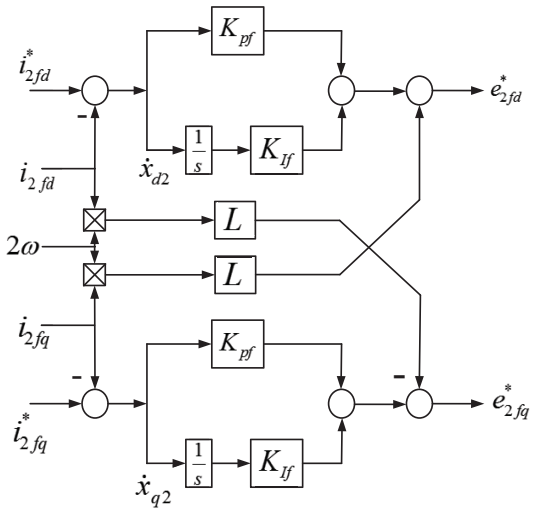


Fig. 3. Scheme for regulation of circulating current.

As Fig. 3 indicates, the reference voltage commands in the $d-q$ reference frame can be written as

$$\begin{bmatrix} e^*_{2fd} \\ e^*_{2fq} \end{bmatrix} = K_{pf}\begin{bmatrix} i^*_{2fd} \\ i^*_{2fq} \end{bmatrix} - K_{pf}\begin{bmatrix} i_{2fd} \\ i_{2fq} \end{bmatrix} + K_{If}\begin{bmatrix} x_{d2} \\ x_{q2} \end{bmatrix} + 2\omega L\begin{bmatrix} i_{2fq} \\ -i_{2fd} \end{bmatrix} \tag{23}$$

Assuming $\xi = 2\omega t$, one can derive the corresponding voltage references for phase $a$ and $b$ as

$$\begin{aligned} e^*_{fa} &= K_{pf}\left(i^*_{2fd}\cos\xi - i^*_{2fq}\sin\xi\right) \\ &- \left(K_{pf} + \frac{2\omega L}{\sqrt{3}}\right)\left(i_{diffa} - \frac{i_{dc}}{3}\right) + K_{If}x_{a2} \\ &- \frac{4\omega L}{\sqrt{3}}\left(i_{diffb} - \frac{i_{dc}}{3}\right) \end{aligned} \tag{24}$$

$$\begin{aligned} e^*_{fb} &= K_{pf}\left\{i^*_{2fd}\cos\left(\xi - \frac{4\pi}{3}\right) - i^*_{2fq}\sin\left(\xi - \frac{4\pi}{3}\right)\right\} \\ &- \left(K_{pf} - \frac{2\omega L}{\sqrt{3}}\right)\left(i_{diffb} - \frac{i_{dc}}{3}\right) \\ &+ K_{If}x_{b2} + \frac{4\omega L}{\sqrt{3}}\left(i_{diffa} - \frac{i_{dc}}{3}\right) \end{aligned} \tag{25}$$

The state variables of the PI compensators, Fig. 3, in the $d-q$ frame are related to the corresponding phase values as

$$\begin{bmatrix} x_{a2} \\ x_{b2} \end{bmatrix} = \begin{bmatrix} \cos\xi & -\sin\xi \\ \cos\left(\xi - \frac{4\pi}{3}\right) & -\sin\left(\xi - \frac{4\pi}{3}\right) \end{bmatrix}\begin{bmatrix} x_{d2} \\ x_{q2} \end{bmatrix} \tag{26}$$

The state-space equations of the PI compensators can be written as

$$\begin{bmatrix} \dot{x}_{d2} \\ \dot{x}_{q2} \end{bmatrix} = \begin{bmatrix} i^*_{2fd} \\ i^*_{2fq} \end{bmatrix} - \begin{bmatrix} i_{2fd} \\ i_{2fq} \end{bmatrix} \tag{27}$$

Transforming the $d$-$q$ frame quantities to $a$ and $b$-phase quantities we get

$$f_{6a} = \frac{dx_{a2}}{dt} = \frac{2\omega}{\sqrt{3}}\left(x_{a2} + 2x_{b2}\right) - \left(i_{diffa} - \frac{i_{dc}}{3}\right) + \left(i^*_{2fd}\cos\xi - i^*_{2fq}\sin\xi\right) \quad (28)$$

$$f_{6b} = \frac{dx_{b2}}{dt} = -\frac{2\omega}{\sqrt{3}}\left(2x_{a2} + x_{b2}\right) - \left(i_{diffb} - \frac{i_{dc}}{3}\right) + \left\{i^*_{2fd}\cos\left(\xi - \frac{4\pi}{3}\right) - i^*_{2fq}\sin\left(\xi - \frac{4\pi}{3}\right)\right\} \quad (29)$$

Equations (28) and (29) will be augmented with equations (9) through (12), (20), and (21) while formulating the nonlinear state-space model.

### C. Control Law

The control commands $\eta^*_{Uj}$ and $\eta^*_{Lj}$ are produced from the control commands $e^*_j$ and $e^*_{fj}$ based on the relations

$$\eta^*_{Uj} = \frac{1}{2} - \frac{e^*_j + e^*_{fj}}{v_{dc}} \quad (30)$$

$$\eta^*_{Lj} = \frac{1}{2} + \frac{e^*_j - e^*_{fj}}{v_{dc}} \quad (31)$$

The following constraints need to be imposed on the control commands

$$0 \le \eta^*_{Uj} \le 1, \qquad 0 \le \eta^*_{Lj} \le 1 \quad (32)$$

### D. State-space Model of AVM with SM Insertion Dynamics

Equations (9) through (12), (20), (21), (28), and (29) constitute a nonlinear state-space model for the MMC of the form $\dot{x} = f(x, u, z)$. These equations were put into boxes in previous sections for ease of identification. Variables $\eta^*_{Uj}$ and $\eta^*_{Lj}$ in equations (9)-(12) are replaced by expressions of $e^*_j$ and $e^*_{fj}$ as in equations (18), (19), (24), (25), (30), and (31). Since there are 6 equations for each phase (phases $a$ and $b$), it leads to 12 state variables ($x$). In addition, there are 4 control variables ($u$) and 4 algebraic variables ($z$). These equations are expressed in a compact form as shown below:

$$\dot{x} = f(x, u, z) \quad (33)$$

$$x = \left[\begin{array}{cccccccc} v_{Ua} & v_{Ub} & v_{La} & v_{Lb} & i_{diffa} & i_{diffb} & \cdots \\ i_a & i_b & x_{a1} & x_{b1} & x_{a2} & x_{b2} \end{array}\right]^T \quad (34)$$

$$u = \left[\begin{array}{cccc} i^*_d & i^*_q & i^*_{2fd} & i^*_{2fq} \end{array}\right]^T \quad (35)$$

$$z = \left[\begin{array}{cccc} v_{ga} & v_{gb} & v_{dc} & i_{dc} \end{array}\right]^T \quad (36)$$

As mentioned before, equations for phases $a$ and $b$ are sufficient for the dynamic model, in view of the assumption (16).

## VI. Proposed Stability Analysis: AVM Considering SM Insertion Dynamics

As described in Section V-D, the state-space model is nonlinear in nature. To do stability analysis, we will linearize this model around an operating point, as described next.

### A. Linearized State-Space Model

The nonlinear state-space model (33) can be linearized around a nominal operating point $(x_0, u_0, z_0)$, and expressed in the form

$$\Delta\dot{x}(t) = A(t)\Delta x(t) + B(t)\Delta u(t) + \Gamma(t)\Delta z(t),$$

$$A(t) \in \Re^{n\times n}, B(t) \in \Re^{n\times m}, \Gamma(t) \in \Re^{n\times p}$$

$$A(t) = \left.\frac{\partial f}{\partial x}\right|_0, B(t) = \left.\frac{\partial f}{\partial u}\right|_0, \Gamma(t) = \left.\frac{\partial f}{\partial z}\right|_0 \quad (37)$$

The subscript '0' is used to signify values at the current operating condition. The non-zero elements of the matrix $A(t)$, $B(t)$, and $\Gamma(t)$ are given below.

***Elements of*** $A(t)$ ***matrix:***

$$A(1,5) = \frac{N}{C}\left\{\eta^*_{Ua0} + \frac{1}{v_{dc0}}\left(\frac{i_{a0}}{2} + i_{diffa0}\right)\left(K_{pf} + \frac{2\omega L}{\sqrt{3}}\right)\right\}$$

$$A(1,6) = \frac{N}{C}\frac{4\omega L}{\sqrt{3}v_{dc0}}\left(\frac{i_{a0}}{2} + i_{diffa0}\right)$$

$$A(1,7) = \frac{N}{C}\left\{\frac{\eta^*_{Ua0}}{2} + \frac{1}{v_{dc0}}\left(\frac{i_{a0}}{2} + i_{diffa0}\right)\left(K_p + \frac{\omega L'}{\sqrt{3}}\right)\right\}$$

$$A(1,8) = \frac{N}{C}\frac{2\omega L'}{\sqrt{3}v_{dc0}}\left(\frac{i_{a0}}{2} + i_{diffa0}\right)$$

$$A(1,9) = -\frac{N}{C}\frac{K_I}{v_{dc0}}\left(\frac{i_{a0}}{2} + i_{diffa0}\right)$$

$$A(1,11) = -\frac{N}{C}\frac{K_{If}}{v_{dc0}}\left(\frac{i_{a0}}{2} + i_{diffa0}\right)$$

$$A(2,5) = -\frac{N}{C}\frac{4\omega L}{\sqrt{3}v_{dc0}}\left(\frac{i_{b0}}{2} + i_{diffb0}\right)$$

$$A(2,6) = \frac{N}{C}\left\{\eta^*_{Ub0} + \frac{1}{v_{dc0}}\left(\frac{i_{b0}}{2} + i_{diffb0}\right)\left(K_{pf} - \frac{2\omega L}{\sqrt{3}}\right)\right\}$$

$$A(2,7) = -\frac{N}{C}\frac{2\omega L'}{\sqrt{3}v_{dc0}}\left(\frac{i_{b0}}{2} + i_{diffb0}\right)$$

$$A(2,8) = \frac{N}{C}\left\{\frac{\eta^*_{Ub0}}{2} + \frac{1}{v_{dc0}}\left(\frac{i_{b0}}{2} + i_{diffb0}\right)\left(K_p - \frac{\omega L'}{\sqrt{3}}\right)\right\}$$

$$A(2,10) = -\frac{N}{C}\frac{K_I}{v_{dc0}}\left(\frac{i_{b0}}{2} + i_{diffb0}\right)$$

$$A(2,12) = -\frac{N}{C}\frac{K_{If}}{v_{dc0}}\left(\frac{i_{b0}}{2} + i_{diffb0}\right)$$

$$A(3,5) = \frac{N}{C}\left\{\eta^*_{La0} + \frac{1}{v_{dc0}}\left(-\frac{i_{a0}}{2} + i_{diffa0}\right)\left(K_{pf} + \frac{2\omega L}{\sqrt{3}}\right)\right\}$$

$$A(3,6) = -\frac{N}{C}\frac{4\omega L}{\sqrt{3}v_{dc0}}\left(-\frac{i_{a0}}{2} + i_{diffa0}\right)$$

$$A(3,7) = \frac{N}{C}\left\{-\frac{\eta^*_{La0}}{2} - \frac{1}{v_{dc0}}\left(-\frac{i_{a0}}{2} + i_{diffa0}\right)\left(K_p + \frac{\omega L'}{\sqrt{3}}\right)\right\}$$

$$A(3,8)=-\frac{N}{C}\frac{2\omega L'}{\sqrt{3}v_{dc0}}\left(-\frac{i_{a0}}{2}+i_{diffa0}\right)$$
$$A(3,9)=\frac{N}{C}\frac{K_I}{v_{dc0}}\left(-\frac{i_{a0}}{2}+i_{diffa0}\right)$$
$$A(3,11)=-\frac{N}{C}\frac{K_{If}}{v_{dc0}}\left(-\frac{i_{a0}}{2}+i_{diffa0}\right)$$
$$A(4,5)=-\frac{N}{C}\frac{4\omega L}{\sqrt{3}v_{dc0}}\left(-\frac{i_{b0}}{2}+i_{diffb0}\right)$$
$$A(4,6)=\frac{N}{C}\left\{\eta^*_{Lb0}+\frac{1}{v_{dc0}}\left(-\frac{i_{b0}}{2}+i_{diffb0}\right)\left(K_{pf}-\frac{2\omega L}{\sqrt{3}}\right)\right\}$$
$$A(4,7)=\frac{N}{C}\frac{2\omega L'}{\sqrt{3}v_{dc0}}\left(-\frac{i_{b0}}{2}+i_{diffb0}\right)$$
$$A(4,8)=\frac{N}{C}\left\{-\frac{\eta^*_{Lb0}}{2}-\frac{1}{v_{dc0}}\left(-\frac{i_{b0}}{2}+i_{diffb0}\right)\left(K_p-\frac{\omega L'}{\sqrt{3}}\right)\right\}$$
$$A(4,10)=\frac{N}{C}\frac{K_I}{v_{dc0}}\left(-\frac{i_{b0}}{2}+i_{diffb0}\right)$$
$$A(4,12)=-\frac{N}{C}\frac{K_{If}}{v_{dc0}}\left(-\frac{i_{b0}}{2}+i_{diffb0}\right)$$
$$A(5,1)=-\frac{\eta^*_{Ua0}}{2L},A(5,3)=-\frac{\eta^*_{La0}}{2L}$$
$$A(5,5)=\frac{1}{L}\left\{-R-\frac{1}{2v_{dc0}}\left(K_{pf}+\frac{2\omega L}{\sqrt{3}}\right)(v_{Ua0}+v_{La0})\right\}$$
$$A(5,6)=-\frac{2\omega}{\sqrt{3}v_{dc0}}(v_{Ua0}+v_{La0})$$
$$A(5,7)=\frac{1}{2L}\frac{1}{v_{dc0}}\left(K_p+\frac{\omega L'}{\sqrt{3}}\right)(-v_{Ua0}+v_{La0})$$
$$A(5,8)=\frac{1}{L}\frac{\omega L'}{\sqrt{3}v_{dc0}}(-v_{Ua0}+v_{La0})$$
$$A(5,9)=\frac{1}{2L}\frac{K_I}{v_{dc0}}(v_{Ua0}-v_{La0})$$
$$A(5,11)=\frac{1}{2L}\frac{K_{If}}{v_{dc0}}(v_{Ua0}+v_{La0})$$
$$A(6,2)=-\frac{\eta^*_{Ub0}}{2L},A(6,4)=-\frac{\eta^*_{Lb0}}{2L}$$
$$A(6,5)=\frac{2\omega}{\sqrt{3}v_{dc0}}(v_{Ub0}+v_{Lb0})$$
$$A(6,6)=\frac{1}{L}\left\{-R-\frac{1}{2v_{dc0}}\left(K_{pf}-\frac{2\omega L}{\sqrt{3}}\right)(v_{Ub0}+v_{Lb0})\right\}$$
$$A(6,7)=\frac{1}{L}\frac{\omega L'}{\sqrt{3}v_{dc0}}(v_{Ub0}-v_{Lb0})$$
$$A(6,8)=\frac{1}{2L}\frac{1}{v_{dc0}}\left(K_p-\frac{\omega L'}{\sqrt{3}}\right)(-v_{Ub0}+v_{Lb0})$$
$$A(6,10)=\frac{1}{2L}\frac{K_I}{v_{dc0}}(v_{Ub0}-v_{Lb0})$$
$$A(6,12)=\frac{1}{2L}\frac{K_{If}}{v_{dc0}}(v_{Ub0}+v_{Lb0})$$
$$A(7,1)=-\frac{\eta^*_{Ua0}}{2L'},A(7,3)=\frac{\eta^*_{La0}}{2L'}$$
$$A(7,5)=\frac{1}{L'}\frac{1}{2v_{dc0}}\left(K_{pf}+\frac{2\omega L}{\sqrt{3}}\right)(v_{La0}-v_{Ua0})$$
$$A(7,6)=\frac{1}{L'}\frac{2\omega L}{\sqrt{3}v_{dc0}}(v_{La0}-v_{Ua0})$$
$$A(7,7)=\frac{1}{L'}\left\{-R'-\frac{1}{2v_{dc0}}\left(K_p+\frac{\omega L'}{\sqrt{3}}\right)(v_{La0}+v_{Ua0})\right\}$$
$$A(7,8)=-\frac{\omega}{\sqrt{3}v_{dc0}}(v_{La0}+v_{Ua0})$$
$$A(7,9)=\frac{1}{2L'}\frac{K_I}{v_{dc0}}(v_{La0}+v_{Ua0})$$
$$A(7,11)=\frac{1}{2L'}\frac{K_{If}}{v_{dc0}}(-v_{La0}+v_{Ua0})$$
$$A(8,2)=-\frac{\eta^*_{Ub0}}{2L'},A(8,4)=\frac{\eta^*_{Lb0}}{2L'}$$
$$A(8,5)=-\frac{1}{L'}\frac{2\omega L}{\sqrt{3}v_{dc0}}(v_{Lb0}-v_{Ub0})$$
$$A(8,6)=\frac{1}{L'}\frac{1}{2v_{dc0}}\left(K_{pf}-\frac{2\omega L}{\sqrt{3}}\right)(v_{Lb0}-v_{Ub0})$$
$$A(8,7)=\frac{\omega}{\sqrt{3}v_{dc0}}(v_{Lb0}+v_{Ub0})$$
$$A(8,8)=\frac{1}{L'}\left\{-R'-\frac{1}{2v_{dc0}}\left(K_p-\frac{\omega L'}{\sqrt{3}}\right)(v_{Lb0}+v_{Ub0})\right\}$$
$$A(8,10)=\frac{1}{2L'}\frac{K_I}{v_{dc0}}(v_{Lb0}+v_{Ub0})$$
$$A(8,12)=\frac{1}{2L'}\frac{K_{If}}{v_{dc0}}(-v_{Lb0}+v_{Ub0})$$
$$A(9,7)=-1,A(9,9)=-\frac{\omega}{\sqrt{3}},A(9,10)=-\frac{2\omega}{\sqrt{3}}$$
$$A(10,8)=-1,A(10,9)=\frac{2\omega}{\sqrt{3}},A(10,10)=\frac{\omega}{\sqrt{3}}$$
$$A(11,5)=-1,A(11,11)=\frac{2\omega}{\sqrt{3}},A(11,12)=\frac{4\omega}{\sqrt{3}}$$
$$A(12,6)=-1,A(12,11)=-\frac{4\omega}{\sqrt{3}},A(12,12)=-\frac{2\omega}{\sqrt{3}}$$

***Elements of*** $B(t)$ ***matrix:***

$$B(1,1)=-\frac{NK_p\cos\rho}{Cv_{dc0}}\left(\frac{i_{a0}}{2}+i_{diffa0}\right)$$
$$B(1,2)=\frac{NK_p\sin\rho}{Cv_{dc0}}\left(\frac{i_{a0}}{2}+i_{diffa0}\right)$$
$$B(1,3)=-\frac{NK_{pf}\cos\xi}{Cv_{dc0}}\left(\frac{i_{a0}}{2}+i_{diffa0}\right)$$
$$B(1,4)=\frac{NK_{pf}\sin\xi}{Cv_{dc0}}\left(\frac{i_{a0}}{2}+i_{diffa0}\right)$$
$$B(2,1)=-\frac{NK_p}{Cv_{dc0}}\left(\frac{i_{b0}}{2}+i_{diffb0}\right)\cos\left(\rho-\frac{2\pi}{3}\right)$$
$$B(2,2)=\frac{NK_p}{Cv_{dc0}}\left(\frac{i_{b0}}{2}+i_{diffb0}\right)\sin\left(\rho-\frac{2\pi}{3}\right)$$
$$B(2,3)=-\frac{NK_{pf}}{Cv_{dc0}}\left(\frac{i_{b0}}{2}+i_{diffb0}\right)\cos\left(\xi-\frac{4\pi}{3}\right)$$
$$B(2,4)=\frac{NK_{pf}}{Cv_{dc0}}\left(\frac{i_{b0}}{2}+i_{diffb0}\right)\sin\left(\xi-\frac{4\pi}{3}\right)$$
$$B(3,3)=-\frac{NK_{pf}\cos\xi}{Cv_{dc0}}\left(-\frac{i_{a0}}{2}+i_{diffa0}\right)$$
$$B(3,4)=\frac{NK_{pf}\sin\xi}{Cv_{dc0}}\left(-\frac{i_{a0}}{2}+i_{diffa0}\right)$$
$$B(4,1)=\frac{NK_p}{Cv_{dc0}}\left(-\frac{i_{b0}}{2}+i_{diffb0}\right)\cos\left(\rho-\frac{2\pi}{3}\right)$$
$$B(4,2)=-\frac{NK_p}{Cv_{dc0}}\left(-\frac{i_{b0}}{2}+i_{diffb0}\right)\sin\left(\rho-\frac{2\pi}{3}\right)$$

$$B(4,3) = -\frac{NK_{pf}}{Cv_{dc0}}\left(-\frac{i_{b0}}{2} + i_{diffb0}\right)\cos\left(\xi - \frac{4\pi}{3}\right)$$
$$B(4,4) = \frac{NK_{pf}}{Cv_{dc0}}\left(-\frac{i_{b0}}{2} + i_{diffb0}\right)\sin\left(\xi - \frac{4\pi}{3}\right)$$
$$B(5,1) = \frac{K_p\cos\rho}{2Lv_{dc0}}\left(v_{Ua0} - v_{La0}\right)$$
$$B(5,2) = \frac{K_p\sin\rho}{2Lv_{dc0}}\left(-v_{Ua0} + v_{La0}\right)$$
$$B(5,3) = \frac{K_{pf}\cos\xi}{2Lv_{dc0}}\left(v_{Ua0} + v_{La0}\right)$$
$$B(5,4) = \frac{K_{pf}\sin\xi}{2Lv_{dc0}}\left(-v_{Ua0} - v_{La0}\right)$$
$$B(6,1) = \frac{K_p}{2Lv_{dc0}}\left(v_{Ub0} - v_{Lb0}\right)\cos\left(\rho - \frac{2\pi}{3}\right)$$
$$B(6,2) = \frac{K_p}{2Lv_{dc0}}\left(-v_{Ub0} + v_{Lb0}\right)\sin\left(\rho - \frac{2\pi}{3}\right)$$
$$B(6,3) = \frac{K_{pf}}{2Lv_{dc0}}\left(v_{Ub0} + v_{Lb0}\right)\cos\left(\xi - \frac{4\pi}{3}\right)$$
$$B(6,4) = \frac{K_{pf}}{2Lv_{dc0}}\left(-v_{Ub0} - v_{Lb0}\right)\sin\left(\xi - \frac{4\pi}{3}\right)$$
$$B(7,1) = \frac{K_p\cos\rho}{2L'v_{dc0}}\left(v_{La0} + v_{Ua0}\right)$$
$$B(7,2) = \frac{K_p\sin\rho}{2L'v_{dc0}}\left(-v_{La0} - v_{Ua0}\right)$$
$$B(7,3) = \frac{K_{pf}\cos\xi}{2L'v_{dc0}}\left(-v_{La0} + v_{Ua0}\right)$$
$$B(7,4) = \frac{K_{pf}\sin\xi}{2L'v_{dc0}}\left(v_{La0} - v_{Ua0}\right)$$
$$B(8,1) = \frac{K_p}{2L'v_{dc0}}\left(v_{Lb0} + v_{Ub0}\right)\cos\left(\rho - \frac{2\pi}{3}\right)$$
$$B(8,2) = \frac{K_p}{2L'v_{dc0}}\left(-v_{Lb0} - v_{Ub0}\right)\sin\left(\rho - \frac{2\pi}{3}\right)$$
$$B(8,3) = \frac{K_{pf}}{2L'v_{dc0}}\left(-v_{Lb0} + v_{Ub0}\right)\cos\left(\xi - \frac{4\pi}{3}\right)$$
$$B(8,4) = \frac{K_{pf}}{2L'v_{dc0}}\left(v_{Lb0} - v_{Ub0}\right)\sin\left(\xi - \frac{4\pi}{3}\right)$$
$$B(9,1) = \cos\rho, B(9,2) = -\sin\rho$$
$$B(10,1) = \cos\left(\rho - \frac{2\pi}{3}\right), B(10,2) = -\sin\left(\rho - \frac{2\pi}{3}\right)$$
$$B(11,3) = \cos\xi, B(11,4) = -\sin\xi$$
$$B(12,3) = \cos\left(\xi - \frac{4\pi}{3}\right), B(12,4) = -\sin\left(\xi - \frac{4\pi}{3}\right)$$

***Elements of*** $\Gamma(t)$ ***matrix:***

$$\Gamma(1,1) = -\frac{N}{Cv_{dc0}}\left(\frac{i_{a0}}{2} + i_{diffa0}\right)$$
$$\Gamma(1,3) = \frac{Ne^*_{a0}}{Cv^2_{dc0}}\left(\frac{i_{a0}}{2} + i_{diffa0}\right)$$
$$\Gamma(1,4) = \frac{N\eta^*_{Ua0}}{3C}$$
$$\Gamma(2,2) = -\frac{N}{Cv_{dc0}}\left(\frac{i_{b0}}{2} + i_{diffb0}\right)$$
$$\Gamma(2,3) = \frac{Ne^*_{b0}}{Cv^2_{dc0}}\left(\frac{i_{b0}}{2} + i_{diffb0}\right)$$
$$\Gamma(2,4) = \frac{N\eta^*_{Ub0}}{3C}$$
$$\Gamma(3,1) = \frac{N}{Cv_{dc0}}\left(-\frac{i_{a0}}{2} + i_{diffa0}\right)$$
$$\Gamma(3,3) = -\frac{Ne^*_{a0}}{Cv^2_{dc0}}\left(-\frac{i_{a0}}{2} + i_{diffa0}\right)$$
$$\Gamma(3,4) = \frac{N\eta^*_{La0}}{3C}$$
$$\Gamma(4,2) = \frac{N}{Cv_{dc0}}\left(-\frac{i_{b0}}{2} + i_{diffb0}\right)$$
$$\Gamma(4,3) = -\frac{Ne^*_{b0}}{Cv^2_{dc0}}\left(-\frac{i_{b0}}{2} + i_{diffb0}\right)$$
$$\Gamma(4,4) = \frac{N\eta^*_{Lb0}}{3C}$$
$$\Gamma(5,1) = \frac{1}{2Lv_{dc0}}\left(v_{Ua0} - v_{La0}\right)$$
$$\Gamma(5,3) = \frac{1}{2L}\left\{1 + \frac{e^*_{a0}}{v^2_{dc0}}\left(-v_{Ua0} + v_{La0}\right)\right\}$$
$$\Gamma(5,4) = -\frac{R}{3L}$$
$$\Gamma(6,2) = \frac{1}{2Lv_{dc0}}\left(v_{Ub0} - v_{Lb0}\right)$$
$$\Gamma(6,3) = \frac{1}{2L}\left\{1 + \frac{e^*_{b0}}{v^2_{dc0}}\left(-v_{Ub0} + v_{Lb0}\right)\right\}$$
$$\Gamma(6,4) = -\frac{R}{3L}$$
$$\Gamma(7,1) = \frac{1}{L'}\left\{-1 + \frac{1}{2v_{dc0}}\left(v_{Ua0} + v_{La0}\right)\right\}$$
$$\Gamma(7,3) = \frac{e^*_{a0}}{2L'v^2_{dc0}}\left(-v_{La0} - v_{Ua0}\right)$$
$$\Gamma(8,2) = \frac{1}{L'}\left\{-1 + \frac{1}{2v_{dc0}}\left(v_{Ub0} + v_{Lb0}\right)\right\}$$
$$\Gamma(8,3) = \frac{e^*_{b0}}{2L'v^2_{dc0}}\left(-v_{Lb0} - v_{Ub0}\right)$$

Next, we will analyze the stability properties of this linearized model.

### *B. Linear Time Periodic Framework & Analysis*

From the expressions of $A(t)$, $B(t)$, and $\Gamma(t)$, it is clear that the elements of these matrices are functions of instantaneous values of different variables (e.g. voltages, currents, and controller state variables). From the physical properties of MMC, it is known that some of these have only fundamental frequency component while others have dc, fundamental, second harmonic components, or a combination thereof. Let the nominal operating condition for phase-$a$ variables be:

$$e^*_{a0} = E_{m0}\cos(\omega t + \theta_{ea0})$$
$$e^*_{fa0} = E_{mf0}\cos(2\omega t + \theta_{efa0})$$
$$i_{a0} = I_{m0}\cos(\omega t + \theta_{ia0})$$
$$i_{diffa0} = \tfrac{i_{dc0}}{3} + I_{2f0}\cos(2\omega t + \varphi_0)$$
$$v_{Ua0} = V_{U00} + V_{U10}\cos(\omega t + \theta_{U10}) + V_{U20}\cos(2\omega t + \theta_{U20})$$
$$v_{La0} = V_{L00} + V_{L10}\cos(\omega t + \theta_{L10}) + V_{L20}\cos(2\omega t + \theta_{L20})$$

Similar expressions can be written for the phase $b$ variables.

Substituting these variables in the expressions of $A(t)$, $B(t)$, and $\Gamma(t)$, it is clear that the linear model is time-varying. Stability analysis of such a linear time-varying (LTV) system is challenging since modal analysis methods, such as eigenvalue analysis used for linear time-invariant (LTI) systems, can not be applied.

It can be seen that the state-space model (37) is primarily $T_A$-periodic with a time-period of $T_A = \frac{\omega}{2\pi}$. Hence, we can categorize this as a Linear Time-Periodic (LTP) system. Therefore, the stability properties of LTP systems [50], [51] can be applied in this case.

For the sake of completeness, one can recall the following definitions and fundamental concepts relating the LTP systems [50], [51]:

*1) Fundamentals of Linear Time-Periodic (LTP) Systems:*

- Periodic Function: *A function is primarily $T_A$-periodic or periodic with primary period $T_A$ if $T_A \in \Re^{+*}$ is the smallest number such that*

$$f(t) = f(t + T_A), \forall t \tag{38}$$

  *where $\Re^{+*}$ denotes the set of real strictly positive numbers.*
- Linear Time-Periodic (LTP) system: A Linear Time-Periodic (LTP) system is characterized by the following representation

$$\Delta\dot{x}(t) = A(t)\Delta x(t) + B(t)\Delta u(t) + \Gamma(t)\Delta z(t),$$
$$\Delta x(t) \in \Re^n, \Delta u(t) \in \Re^m, \Delta z(t) \in \Re^p$$

  Here, the elements of matrices $A(t)$, $B(t)$, and $\Gamma(t)$ are known, real-valued, piecewise continuous, primarily $T_A$-periodic functions defined on $\Re^+$.
- Fundamental Matrix: Any nonsingular solution of the homogeneous differential system $\Delta\dot{x}(t) = A(t)\Delta x(t)$ is known as its Fundamental Matrix.
- State Transition Matrix (STM): There exists a unique fundamental matrix $\Phi(t, t_0)$ of the homogeneous system mentioned above, such that $\Phi(t_0, t_0) = I$. This matrix is called the State Transition Matrix (STM) of the system. Without any loss of generality, we shall assume $t_0 = 0$.
- Monodromy Matrix: The STM computed after one time-period $T_A$, i.e. $\Phi(T_A, 0)$ is known as the Monodromy Matrix.
- Poincaré multipliers: The eigenvalues of the Monodromy matrix are called the Poincaré multipliers.

For the stability analysis of the LTP systems, it is essential to calculate the state-transition matrix (STM) $\Phi(\cdot, 0)$. In most cases, the STM can not be computed in closed form. Fortunately, the computation of a monodromy matrix $\Phi(T_A, 0)$, which is essentially the STM after one time-period $T_A$, suffices for stability analysis.

The monodromy matrix $\Phi(T_A, 0)$ can be calculated by numerically solving the equation $\Delta\dot{x}(t) = A(t)\Delta x(t)$ with $n$ different initial conditions $x_r(0) = \epsilon_r, r = 1, 2, \ldots n$, where $\epsilon_r = [\delta_{ri}]$ is the $r^{th}$ column of the identity matrix $I$ [50]. Let $x_r(T_A)$, $r = 1, 2, ..., n$, be the $n$ independent solutions obtained for each initial condition. Then the monodromy matrix is given by:

$$\Phi(T_A, 0) = \begin{bmatrix} x_1(T_A) & x_2(T_A) & \ldots & x_n(T_A) \end{bmatrix} \tag{39}$$

*As mentioned above, the eigenvalues of the monodromy matrix are called the Poincaré multipliers. For an asymptotically stable system, the Poincaré multipliers lie within the unit circle.*

Therefore, the steps for conducting stability analysis of the proposed MMC model are summarized as follows:

- *Step I:* Derive the nonlinear state-space AVM of MMC as described in equation (33).
- *Step II:* Develop the Linear Time-Periodic (LTP) model of the MMC by linearizing the nonlinear AVM obtained from Step I around an operating condition $(x_0, u_0, z_0)$ as shown in equaion (37).
- *Step III:* Calculate the monodromy matrix $\Phi(T_A, 0)$ by numerical integration of $\Delta\dot{x}(t) = A(t)\Delta x(t)$ with $n$ different initial conditions $x_r(0) = \epsilon_r, r = 1, 2, \ldots n$, where $\epsilon_r = [\delta_{ri}]$ is the $r^{th}$ column of the identity matrix $I$ [50]. This has been described before in more details.
- *Step IV:* Compute the Poincaré multipliers, i.e. the eigenvalues of the monodromy matrix $\Phi(T_A, 0)$.
- *Step V:* If the largest magnitude of the Poincaré multiplier is less than unity, then the MMC is considered asymptotically stable.

## VII. Case Study

### A. Test System

The test system consists of a 401-level, 1000-MW, ±320-kV MMC, Fig. 1, with the following parameters:

$$Rated\ MVA = 1059MVA, N = 400, C = 10\ mF,$$
$$L = 50\ mH, R = 0.5236\ \Omega,$$
$$L_t = 60\ mH, R_t = 0.5236\ \Omega.$$

### B. Benchmarking the AVM with SM Insertion Dynamics

The proposed nonlinear AVM of the MMC was described in Section V and the state-space model was presented in a compact form in subsection V-D. These differential equations was implemented using basic math blocks from MATLAB/Simulink library and its response was benchmarked against a detailed model built in PSCAD/EMTDC. The detailed model considers individual SMs and the voltage balancing control for all 400 SMs per arm. The MMC simulation model was developed in PSCAD/EMTDC in the following way:

- The converter leg was modeled by two dependent voltage sources, two resistances and two inductances. The terminal voltage is connected to the ac grid through a leakage reactance;
- Each dependent voltage source in the arm is controlled by a hosted code that reads the arm currents and computes the voltage of each submodule, generating the control signal for the dependent voltage sources and forming the final arm voltage. The hosted code has a 500 kHz sample frequency, allowing a high accuracy in the digital computation;

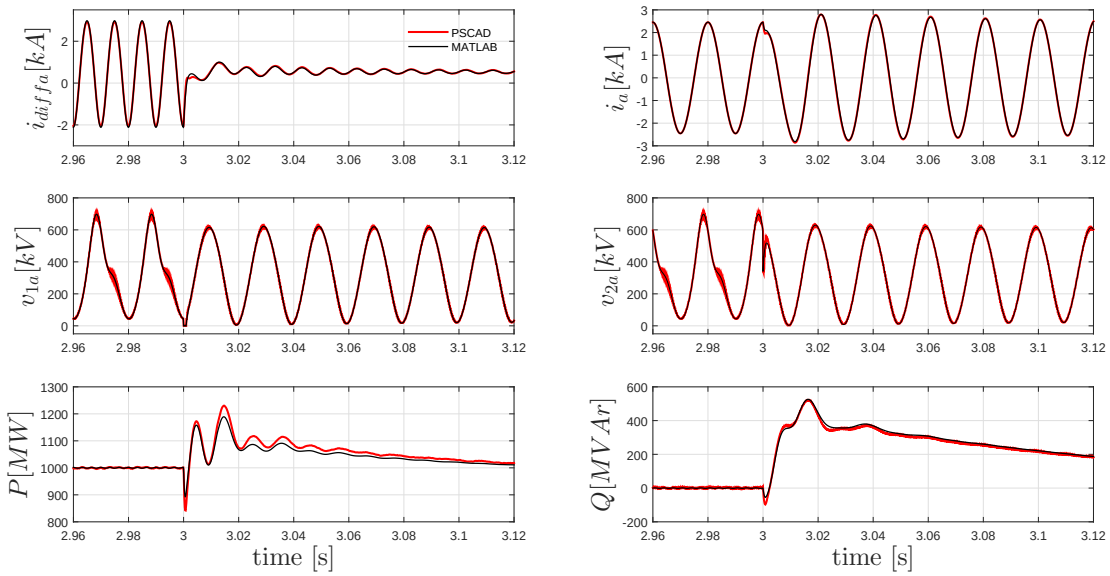


Fig. 4. Comparison of the response between the detailed model in PSCAD/EMTDC against a nonlinear averaged model in MATLAB/Simulink. The circulating current controller is enabled at $t = 3.0$ s.

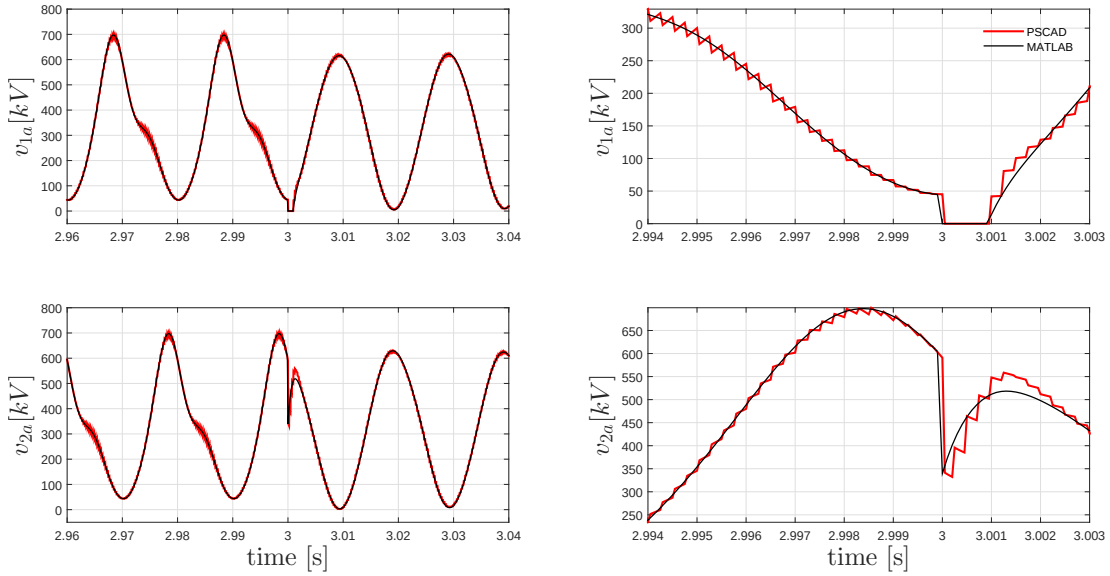


Fig. 5. Zoomed view of the response from the detailed model in PSCAD/EMTDC, compared against a nonlinear averaged model in MATLAB/Simulink. The circulating current controller is enabled at $t = 3.0$ s.

- The simulation model results were compared to other simulation models where each submodule was created by conventional electronic components from PSCAD library, for $M = 4, 6, 8, 10$, and 20, showing negligible error;
- Then, the simulation model was augmented for $M = 400$, in order to simulate the system mentioned in the present paper.

*Such a benchmarking analysis gives us the confidence in the accuracy of the AVM and any stability analysis that is performed by linearizing such models.*

The converter was assumed to control the real power ($P$) and the reactive power ($Q$) at the PCC, Fig. 1. The PI compensator parameters for the output current control scheme and the circulating current control scheme were calculated using the following equations:

$$K_p = \frac{L'}{\tau}, \quad K_I = \frac{R'}{\tau}, \quad K_{pf} = \frac{L}{\tau_f}, \quad K_{If} = \frac{R}{\tau_f}$$

For benchmarking studies, $\frac{1}{\tau} = 500\ s^{-1}$ and $\frac{1}{\tau_f} = 2000\ s^{-1}$ was chosen.

*1) Enabling Circulating Current Control:* The response of different variables obtained from the nonlinear averaged model (black trace) is compared against the detailed model (red trace) in Fig. 4. During $t = 0 - 3.0$ s, the circulating current controller is not activated. It can be seen that the converter is controlling the real power $P$ at 1000 MW at unity power factor. The circulating current $i_{diffa}$ has a dc component and a double frequency component. As expected, the phase current

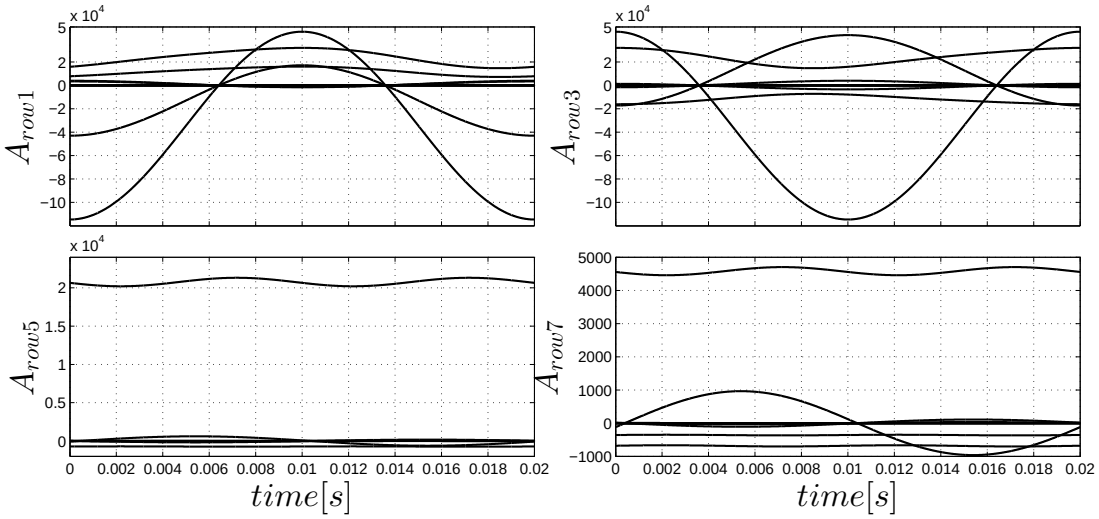


Fig. 6. Time periodic nature of the elements of the A matrix in the linear model. Trajectories of the elements of the first, third, fifth, and seventh rows are shown.

$i_a$ does not have any harmonics. The voltages across the upper and lower arm SMs that are turned ON, $v_{1a}$ and $v_{2a}$, have second and third harmonics. It can be seen that, under steady state, the dotted traces and the solid traces overlap almost indistinguishably.

At $t = 3.0$ s, the circulating current controller is enabled. The controller suppresses the second harmonic component and only the dc component remains in $i_{diffa}$. Following the transients at $t = 3.0$ s, harmonic content in voltages $v_{1a}$ and $v_{2a}$ are significantly reduced. It can also be observed that the circulating current control scheme is not completely decoupled from the output current control scheme. Transients in real power $P$, reactive power $Q$, and phase current $i_a$ can be observed. It can be seen that the response of the averaged model very closely matches that of the detailed model.

The zoomed view of $v_{1a}$ and $v_{2a}$ are shown in Fig. 5. One can appreciate the close match between these models from this figure. It can also be observed that the detailed model inserts the SMs in a discrete manner as opposed to the averaged model that treats the insertion of SMs as a continuous function.

### C. Stability Analysis

*1) Eigen Analysis of Phasor-based AVM:* As described in sections III-B and IV, stability of phasor-based AVM can be analyzed through eigenvalue analysis. Considering $\frac{1}{\tau} = 500\ s^{-1}$, eigenvalues were obtained from the state matrix shown in equation (7). The eigenvalues are: $\lambda = [-500.0000 - 36.9599 - 382.2588 - 154.7011]$. Please note that the eigenvalues are real, stable, and independent of the circulating current controller gains.

*2) Stability Analysis of AVM Considering SM Insertion Dynamics:* The nonlinear averaged model was linearized for stability analysis. As mentioned in Section VI, the first step in this process is to obtain a steady-state operating condition. In this case, the steady-state condition $(x_0, u_0, z_0)$ was obtained by numerical integration of (33) under $P = 1000$ MW and $Q = 0$ MVAr with the circulating current controller enabled. The values of the variables needed for computing matrix $A$ of the linearized model are:

$e^*_{a0} = 276.60cos(\omega t + 0.14)$
$e^*_{fa0} = 19.35\cos(2\omega t - 4.63)$
$i_{a0} = 2.45cos(\omega t)$
$i_{diffa0} = 0.5250$
$v_{Ua0} = 634.37 + 50.01cos(\omega t - 1.70) + 16.95cos(2\omega t - 4.52)$
$v_{La0} = 634.37 + 50.01cos(\omega t + 1.44) + 16.95cos(2\omega t - 4.52)$

where the angles are expressed in radians, voltages are in kV, and currents are in kA. The values of the phase-$b$ quantities can be determined considering appropriate phase difference.

Under this nominal condition, the periodic nature of the elements of the first, third, fifth, and seventh row of matrix $A$ are illustrated in Fig. 6. The monodromy matrix was computed through numerical integration as mentioned in Section VI-B. The corresponding Poincaré multipliers are:

$$\begin{aligned}\mu = [&0.8717 + 0.0000\text{j} \quad 0.8427 + 0.0000\text{j}\ldots\\ &0.8380 \pm 0.0655\text{j} \quad 0.1437 + 0.0000\text{j}\ldots\\ &0.0066 \pm 0.1032\text{j} \quad 0.0130 + 0.0000\text{j}\ldots\\ &-0.0007 \pm 0.0006\text{j} \quad -0.0000 \pm 0.0000\text{j}]^{\mathrm{T}}\end{aligned}$$

Therefore, the system is stable as the multipliers lie within the unit circle.

Next, the value of the PI controller parameters were changed by varying the value of $\frac{1}{\tau_f}$. The locus of the maximum value of the magnitude of the Poincaré multipliers with respect to $\frac{1}{\tau_f}$ is shown in Fig. 7. The operating condition corresponds to $P = 1000$ MW, $Q = 0$ MVAr. It can be seen that an increase in the value from $2000\ s^{-1}$ to $4400\ s^{-1}$ moves the maximum value of the magnitude of the Poincaré multipliers towards the perimeter of the unit circle.

The value of $\frac{1}{\tau_f}$ was set to $5000\ s^{-1}$ and the simulation was run for the condition $P = 1000$ MW, $Q = 0$ MVAr. At $t = 3.0$ s, the circulating current controller is enabled. Figure 8 shows the instability under such a scenario. The averaged model and

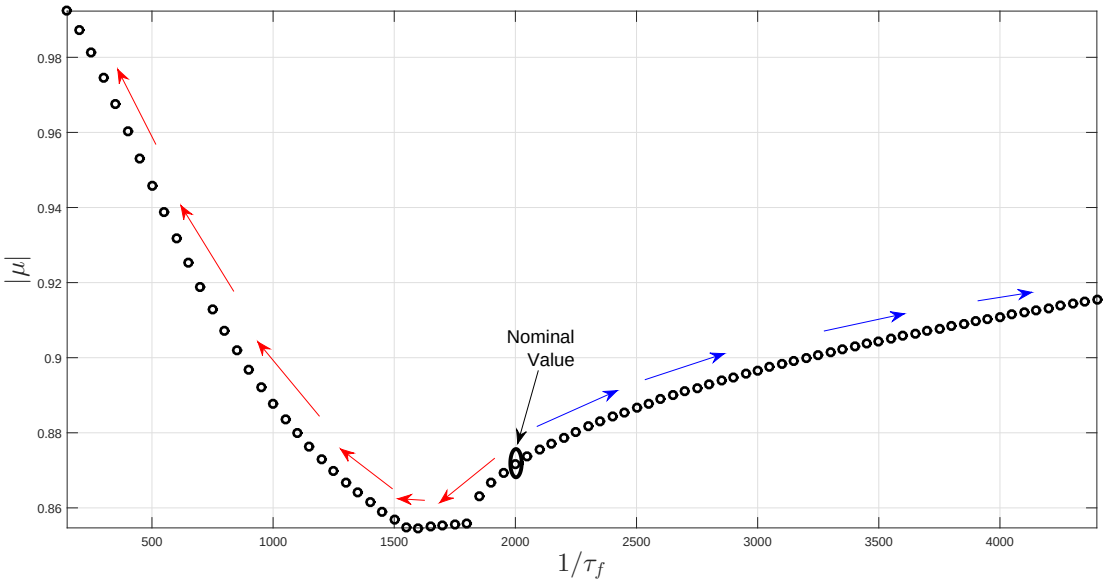


Fig. 7. Locus of the maximum value of the magnitude of the Poincaré multipliers with respect to $\frac{1}{\tau_f}$. The operating condition corresponds to $P = 1000$ MW, $Q = 0$ MVAr.

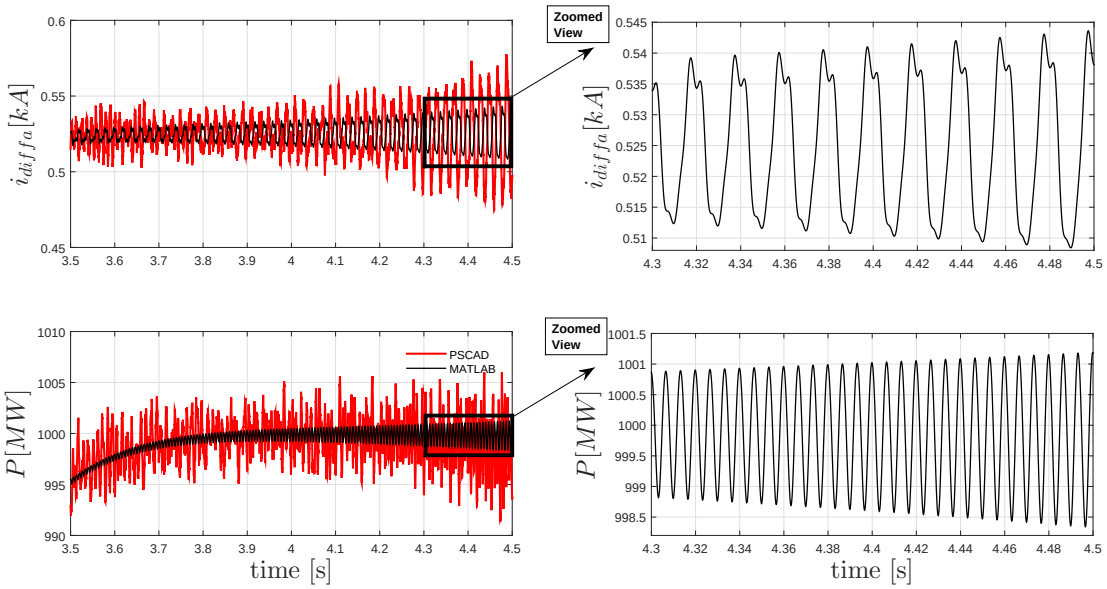


Fig. 8. Comparison of response between the detailed model in PSCAD/EMTDC against a nonlinear averaged model in MATLAB/Simulink. Instability is observed in the response when $\frac{1}{\tau_f}$ is set to $5000\ s^{-1}$. The operating condition corresponds to $P = 1000$ MW, $Q = 0$ MVAr. At $t = 3.0$ s, the circulating current controller is enabled.

the detailed model both demonstrate this phenomena.

When the value of $\frac{1}{\tau_f}$ is reduced from $2000\ s^{-1}$, it can be seen from Fig. 7 that the maximum value of $|\mu|$ reduces and becomes minimum just above $1500\ s^{-1}$. As $\frac{1}{\tau_f}$ is reduced further, the system approaches instability. Figure 9 shows the response obtained from the averaged model. Instability is observed in the response when $\frac{1}{\tau_f}$ is set to $150\ s^{-1}$, with the operating point corresponding to $P = 1000$ MW, $Q = 0$ MVAr. At $t = 3.0$ s, the circulating current controller is enabled.

## VIII. Conclusion

A framework for stability analysis of the MMC is presented based on the Linear Time-Periodic nature of the proposed model. It has been shown that the proposed framework can indicate the zones of instability for certain gains of the circulating current controller, which can not be captured by the traditional eigenvalue analysis of phasor-based AVM.

## IX. Acknowledgement

The authors would like to thank the anonymous reviewers for their constructive comments, which were very helpful in improving the quality of the paper.

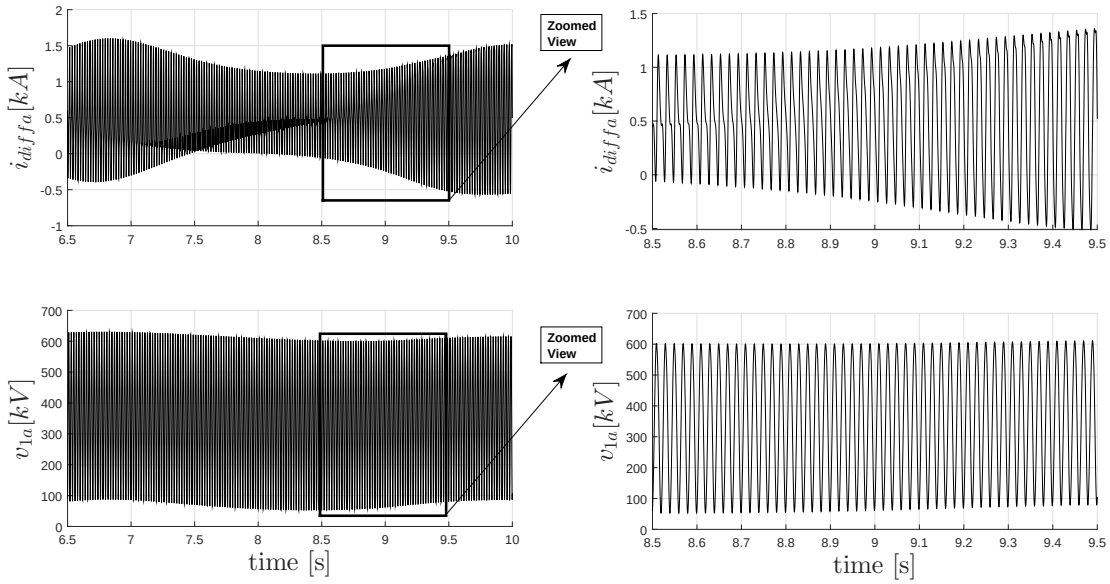


Fig. 9. Response obtained from the averaged model. Instability is observed in the response when $\frac{1}{\tau_f}$ is set to 150 $s^{-1}$. The operating condition corresponds to $P = 1000$ MW, $Q = 0$ MVAr. At $t = 3.0$ s, the circulating current controller is enabled.

## REFERENCES


[1] A. Lesnicar and R. Marquardt, "An Innovative Modular Multilevel Converter Topology Suitable for a Wide Power Range" *IEEE PTC Conference 2003*, vol. 3, Jun. 2003.

[2] Perez, M.A.; Bernet, S.; Rodriguez, J.; Kouro, S.; "Editorial Special Issue on Modular Multilevel Converters," IEEE Transactions on Power Electronics, vol.30, no.1, pp. 1-3, Jan. 2015.

[3] Xiaofeng Yang; Jianghong Li; Xiaopeng Wang; Wenbao Fan; Zheng, T.Q., "Circulating Current Model of Modular Multilevel Converter," 2011 Asia-Pacific Power and Energy Engineering Conference (APPEEC), vol., no., pp.1-6, 25-28 March 2011.

[4] Kolb, J.; Kammerer, F.; Braun, M., "Straight forward vector control of the Modular Multilevel Converter for feeding three-phase machines over their complete frequency range," IECON 2011 - 37th Annual Conference on IEEE Industrial Electronics Society , vol., no., pp.1596-1601, 7-10 Nov. 2011.

[5] Kolb, J.; Kammerer, F.; Gommeringer, M.; Braun, M., "Cascaded Control System of the Modular Multilevel Converter for Feeding Variable-Speed Drives," IEEE Transactions on Power Electronics, vol.30, no.1, pp.349-357, Jan. 2015.

[6] Munch, P.; Gorges, D.; Izak, M.; Liu, Steven, "Integrated current control, energy control and energy balancing of Modular Multilevel Converters," IECON 2010 - 36th Annual Conference on IEEE Industrial Electronics Society , vol., no., pp.150-155, 7-10 Nov. 2010.

[7] Munch, P.; Liu, Steven; Ebner, G., "Multivariable current control of Modular Multilevel Converters with disturbance rejection and harmonics compensation," 2010 IEEE International Conference on Control Applications (CCA), vol., no., pp.196-201, 8-10 Sept. 2010.

[8] Siemaszko, D.; Antonopoulos, A.; Ilves, K.; Vasiladiotis, M.; Angquist, Lennart; Nee, H.-P., "Evaluation of control and modulation methods for modular multilevel converters," 2010 International Power Electronics Conference (IPEC), vol., no., pp.746-753, 21-24 June 2010.

[9] Lachichi, A.; Harnefors, L., "Comparative analysis of control strategies for modular multilevel converters," 2011 IEEE Ninth International Conference on Power Electronics and Drive Systems (PEDS), vol., no., pp.538-542, 5-8 Dec. 2011.

[10] Ilves, Kalle; Antonopoulos, A.; Harnefors, Lennart; Norrga, Staffan; Nee, H.-P., "Circulating current control in modular multilevel converters with fundamental switching frequency," 2012 7th International Power Electronics and Motion Control Conference (IPEMC), vol.1, no., pp.249-256, 2-5 June 2012.

[11] Solas, E.; Abad, G.; Barrena, J.A.; Carcar, A.; Aurtenetxea, S., "Modelling, simulation and control of Modular Multilevel Converter," 2010 14th International Power Electronics and Motion Control Conference (EPE/PEMC), vol., no., pp.T2 90-96, 6-8 Sept. 2010.

[12] Perez, M.A.; Rodriguez, J., "Generalized modeling and simulation of a modular multilevel converter," 2011 IEEE International Symposium on Industrial Electronics (ISIE), vol., no., pp.1863-1868, 27-30 June 2011.

[13] Perez, M.A.; Lizana F, R.; Rodriguez, J., "Decoupled current control of modular multilevel converter for HVDC applications," 2012 IEEE International Symposium on Industrial Electronics (ISIE), vol., no., pp.1979-1984, 28-31 May 2012.

[14] Zhao Yan; Hu Xue-hao; Tang Guang-fu; He Zhi-yuan, "A study on MMC model and its current control strategies," 2010 2nd IEEE International Symposium on Power Electronics for Distributed Generation Systems (PEDG), vol., no., pp.259-264, 16-18 June 2010.

[15] Engel, S.P.; De Doncker, R.W., "Control of the Modular Multi-Level Converter for minimized cell capacitance," Proceedings of the 2011-14th European Conference on Power Electronics and Applications (EPE 2011), vol., no., pp.1-10, Aug. 30 2011-Sept. 1 2011.

[16] Rohner, S.; Bernet, S.; Hiller, M.; Sommer, R., "Modelling, simulation and analysis of a Modular Multilevel Converter for medium voltage applications," 2010 IEEE International Conference on Industrial Technology (ICIT), vol., no., pp.775-782, 14-17 March 2010.

[17] Rohner, S.; Weber, J.; Bernet, S., "Continuous model of Modular Multilevel Converter with experimental verification," 2011 IEEE Energy Conversion Congress and Exposition (ECCE), vol., no., pp.4021-4028, 17-22 Sept. 2011.

[18] U.N. Gnanarathna, A. M. Gole and R. P. Jayasinghe, "Efficient Modeling of Modular Multilevel HVDC Converters (MMC) on Electromagnetic Transient Simulation Programs," *IEEE Transactions on Power Delivery*, vol. 26, no. 1, pp. 316-324, Jan. 2011.

[19] F. Ajaei and R. Iravani, "Enhanced Equivalent Model of the Modular Multilevel Converter," *IEEE Transactions on Power Delivery*, 2014.

[20] O. Venjakob, S. Kubera, R. Hibberts-Caswell, P.A. Forsyth, T.L. Maguire, "Setup and Performance of the Real-Time Simulator used for Hardware-in-Loop-Tests of a VSC-Based HVDC scheme for Offshore Applications", Proceedings of the International Conference on Power Systems Transients (IPST'13) in Vancouver, Canada July 18-20, 2013.

[21] H. Saad, S. Dennetiere, J. Mahseredjian, P. Delarue, X. Guillaud, J. Peralta, and S. Nguefeu, "Modular multilevel converter models for electromagnetic transient," IEEE Trans. on Power Delivery, vol. 29, no. 3, pp. 1481 - 1489, July 2013.

[22] Ludois, D.C.; Venkataramanan, G.; "Simplified Terminal Behavioral Model for a Modular Multilevel Converter," IEEE Transactions on Power Electronics, vol.29, no.4, pp. 1622-1631, April 2014.

[23] Vasiladiotis, M.; Cherix, N.; Rufer, A.; "Accurate Capacitor Voltage Ripple Estimation and Current Control Considerations for Grid- Connected Modular Multilevel Converters," IEEE Transactions on Power Electronics, vol.29, no.9, pp. 4568-4579, Sep. 2014.

[24] Riar, B.S.; Geyer, T.; Madawala, U.K.; "Model Predictive Direct Current Control of Modular Multilevel Converters: Modeling, Analysis, and

Experimental Evaluation," IEEE Transactions on Power Electronics, vol.30, no.1, pp. 431-439, Jan. 2015.
[25] Riar, B.S.; Madawala, U.K.; "Decoupled Control of Modular Multilevel Converters Using Voltage Correcting Modules," Power Electronics, IEEE Transactions on, vol.30, no.2, pp. 690-698, Feb. 2015.
[26] S. Norrga, L. Angquist, K. Ilves, L. Harnefors, and H.-P. Nee, "Frequency-domain modeling of modular multilevel converters," in Proc. 38th Annu. Conf. IEEE Ind. Electron. Soc., Oct. 2528, 2012, pp. 49674972.
[27] Teeuwsen, S.P., "Simplified dynamic model of a voltage-sourced converter with modular multilevel converter design," IEEE/PES Power Systems Conference and Exposition, 2009. PSCE '09. vol., no., pp.1-6, 15-18 March 2009.
[28] Working Group on Modeling and Analysis of System Transients Using Digital Programs, "Dynamic Averaged and Simplified Models for MMC-Based HVDC Transmission Systems," *IEEE Transactions on Power Delivery*, vol. 28, no. 3, pp. 1723-1730, July. 2013.
[29] Cigre Working group B4.57 guide for MMC modelling (document 604).
[30] A. Antonopoulos, L. Angquist and H.P. Nee,"On Dynamics and Voltage Control of the Modular Multilevel Converter," *in Proc. Eur. Conf. Power Electron. Appl., Barcelona, Spain, 2009.*
[31] A. Antonopoulos, L. Angquist, L. Harnefors, K. Ilves and H.P. Nee,"Global Asymptotic Stability of Modular Multilevel Converter," *IEEE Transactions on Industrial Electronics*, vol. 61, no. 2, pp. 603-612, Feb. 2014.
[32] Harnefors, L.; Antonopoulos, A.; Norrga, S.; Angquist, L.; Nee, H.-P., "Dynamic Analysis of Modular Multilevel Converters," *IEEE Transactions on Industrial Electronics*, vol.60, no.7, pp.2526-2537, July 2013.
[33] Harnefors, L.; Norrga, S.; Antonopoulos, A.; Nee, H.-P., "Dynamic modeling of modular multilevel converters," Proceedings of the 2011-14th European Conference on Power Electronics and Applications (EPE 2011), vol., no., pp.1-10, Aug. 30 2011-Sept. 1 2011.
[34] Hagiwara, M.; Maeda, R.; Akagi, H., "Control and Analysis of the Modular Multilevel Cascade Converter Based on Double-Star Chopper-Cells (MMCC-DSCC)," IEEE Transactions on Power Electronics, vol.26, no.6, pp.1649-1658, June 2011.
[35] M. Hagiwara and H. Akagi, "PWM control and experiment of modular multilevel converter," in Proc. IEEE Power Electron. Specialists Conf., Tokyo, Japan, Jun. 2008, pp. 154161.
[36] M. Saeedifard and R. Iravani, Dynamic performance of a modular multilevel back-to-back HVDC system, IEEE Trans. Power Del., vol. 25, no. 4, pp. 29032912, Oct. 2010.
[37] E. Solas, G. Abad, J. A. Barrena, A. Carcar, and S. Aurtenetxea, "Modulation of modular multilevel converter for HVDC application," in Proc. 14th Int. Power Electron. Mot. Control Conf., Mondragon, Spain, Sep. 2010, pp. 8489.
[38] Meshram, P.M.; Borghate, V.B.; "A Simplified Nearest Level Control (NLC) Voltage Balancing Method for Modular Multilevel Converter (MMC)," IEEE Transactions on Power Electronics, vol.30, no.1, pp. 450-462, Jan. 2015.
[39] Siemaszko, D.; "Fast Sorting Method for Balancing Capacitor Voltages in Modular Multilevel Converters," IEEE Transactions on Power Electronics, vol.30, no.1, pp. 463-470, Jan. 2015.
[40] Fujin Deng; Zhe Chen; "A Control Method for Voltage Balancing in Modular Multilevel Converters," IEEE Transactions on Power Electronics, vol.29, no.1, pp. 66-76, Jan. 2014.
[41] Shengfang Fan; Kai Zhang; Jian Xiong; Yaosuo Xue; "An Improved Control System for Modular Multilevel Converters with New Modulation Strategy and Voltage Balancing Control," IEEE Transactions on Power Electronics, vol.30, no.1, pp. 358-371, Jan. 2015.
[42] Fujin Deng; Zhe Chen; "Elimination of DC-Link Current Ripple for Modular Multilevel Converters With Capacitor Voltage-Balancing Pulse-Shifted Carrier PWM," IEEE Transactions on Power Electronics, vol.30, no.1, pp. 284-296, Jan. 2015.
[43] Q. Tu, Z. Xu, and L. Xu "Reduced Switching-Frequency Modulation and Circulating Current Suppression for Modular Multilevel Converters," *IEEE Transactions on Power Delivery*, vol. 23, no. 3, pp. 2009-2017, July. 2011.
[44] Darus, R.; Pou, J.; Konstantinou, G.; Ceballos, S.; Agelidis, V.G., "Circulating current control and evaluation of carrier dispositions in modular multilevel converters," 2013 IEEE ECCE Asia Downunder (ECCE Asia), vol., no., pp.332-338, 3-6 June 2013.
[45] Shaohua Li; Xiuli Wang; Zhiqing Yao; Tai Li; Zhong Peng; "Circulating Current Suppressing Strategy for MMC-HVDC Based on Nonideal Proportional Resonant Controllers Under Unbalanced Grid Conditions," IEEE Transactions on Power Electronics, vol.30, no.1, pp. 387-397, Jan. 2015.
[46] Pou, J.; Ceballos, S.; Konstantinou, G.; Agelidis, V.G.; Picas, R.; Zaragoza, J., "Circulating Current Injection Methods Based on Instantaneous Information for the Modular Multilevel Converter," IEEE Transactions on Industrial Electronics, vol.62, no.2, pp.777-788, Feb. 2015.
[47] Liqun He; Kai Zhang; Jian Xiong; Shengfang Fan; "A Repetitive Control Scheme for Harmonic Suppression of Circulating Current in Modular Multilevel Converters," IEEE Transactions on Power Electronics, vol.30, no.1, pp. 471-481, Jan. 2015.
[48] Ming Zhang; Long Huang; Wenxi Yao; Zhengyu Lu; "Circulating Harmonic Current Elimination of a CPS-PWM-Based Modular Multilevel Converter With a Plug-In Repetitive Controller," IEEE Transactions on Power Electronics, vol.29, no.4, pp. 2083-2097, April 2014.
[49] A. Yazdani, and R. Iravani "Voltage-sourced converters in power systems : modeling, control, and applications," IEEE press, John Wiley and Sons, 1st edition, 2010.
[50] M. Montagnier, R.J. Spiteri, and J. Angeles,"The Control of Linear Time-Periodic Systems with Floquet-Lyapunov Theory," *International Journal of Control*, vol. 77, no. 5, pp. 472-490, Jan. 2004.
[51] Wilson J. Rugh "Linear System Theory," Prentice-Hall information and systems sciences series, Prentice Hall, 1993.

**Nilanjan Ray Chaudhuri** (S'08-M'09) Nilanjan Ray Chaudhuri received his Ph.D. degree from Imperial College London, London, UK in 2011 in Power Systems. From 2005-2007, he worked in General Electric (GE) John F. Welch Technology Center. He came back to GE and worked in GE Global Research Center, NY, USA as a Lead Engineer during 2011-2014. Presently, he is an Assistant Professor with North Dakota State University (NDSU), Fargo, ND, USA. He is a member of the *IEEE, IEEE PES*, and *Sigma Xi*. Dr. Ray Chaudhuri is the lead author of the book *Multi-terminal Direct Current Grids: Modeling, Analysis, and Control* (Wiley/IEEE Press, 2014), and an Associate Editor of the IEEE TRANSACTIONS ON POWER DELIVERY.

**Rafael Oliveira** received his BSc in Control and Automation Engineering and MSc in Electrical Engineering in 2003 and 2005, respectively, from Pontifica Univeridade Catolica do Rio Grande do Sul, Brazil. He is currently a PhD candidate in the Electrical Engineering Program at Ryerson University, Canada. His main area of research is power converters for power systems applications, including simulation, control and modelling.

**Amirnaser Yazdani** (SM'09) received the Ph.D. degree in electrical engineering from the University of Toronto, Toronto, ON, Canada, in 2005. He was an Assistant Professor with the University of Western Ontario (UWO), London, ON. He is currently an Associate Professor at Ryerson University, Toronto. His research interests include modeling and control of electronic power converters, renewable electric power systems, distributed generation and storage, and microgrids. He is a co-author of the book Voltage-Sourced Converters in Power Systems (IEEE-Wiley Press, 2010), and an Associate Editor of the IEEE TRANSACTIONS ON SUSTAINABLE ENERGY.